Plenary Lecture | Plenary lecture

Plenary lecture V

Fri. Jul 19, 2024 9:15 AM - 10:15 AM Room A

[P5-01] Introduction, history, and applications of all speed Riemann flux schemes

*Eiji Shima[1] (1. JAXA)

Keywords: scheme, all-speed Riemann flux, JAXA's research

Introduction, history, and applications of all-speed Riemann flux schemes

Eiji SHIMA

Aeronautical Technology Department

Japan Aerospace Exploration Agency (JAXA)

Outline

1. Background and overview
2. Introduction of JAXA and the applications of SLAU type schemes in JAXA's research projects
3. History and theories of SLAU type scheme
    1. What is the Riemann Flux?
    2. Toward the AUSM type schemes
    3. Toward the SLAU type schemes
4. The implicit time integration scheme for all Ma
5. Future challenges

Background

•As all real fluids are compressible, the compressible Navier-Stokes equation is theoretically a governing equation for flows at all Ma(Mach number) and sound propagation, however, there were problems to apply to the low Ma flows.

•The Godunov-type CFD schemes for compressible flows, in which the Riemann flux function computes the flux at the cell interface, are fundamental for modern high-resolution CFD methods used as the workhouse for the aerospace engineering.

•Recent advancements in the all-speed Riemann flux functions make it possible to compute flows in a broad range of Ma and to cover most aerospace applications.

•SLAU(Simple Low Dissipative Advection Upstream Splitting Method) type schemes we have developed are widely used as the all-speed Riemann flux scheme due to their robustness, simplicity and versatility.

Overview

•The theories of the SLAU type schemes are presented along the history of progress from my point of view.

•I will emphasize the physical images of the schemes. It was helpful to improve the schemes.

• Application of the schemes at JAXA are shown for illustrating the use of SLAU type schemes and its wide range of applications. This also serves as an overview of JAXA's fluid-dynamic and aerodynamic researches.
(There are many other applications those don't use these schemes, of course.)

•Note that the simplified history I will talk about is not a whole history. There have been many excellent researches in this field, e.g. preconditioning methods, that I can't mention.

About JAXA

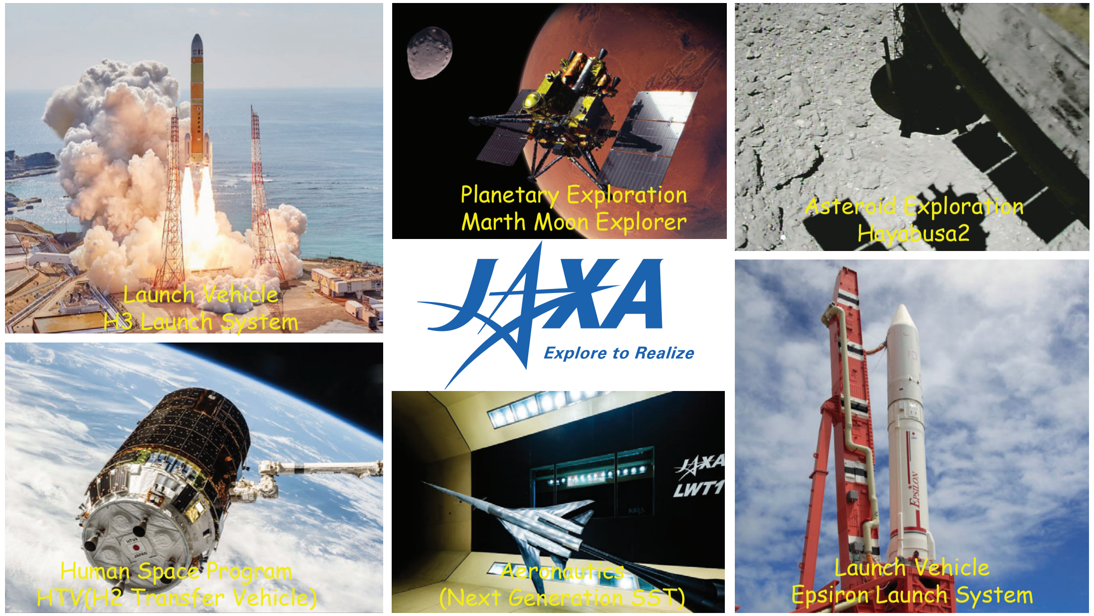

Field Centers

Employees: 1,600 (April 1st, 2023)
78%: technical, 22%: administrative

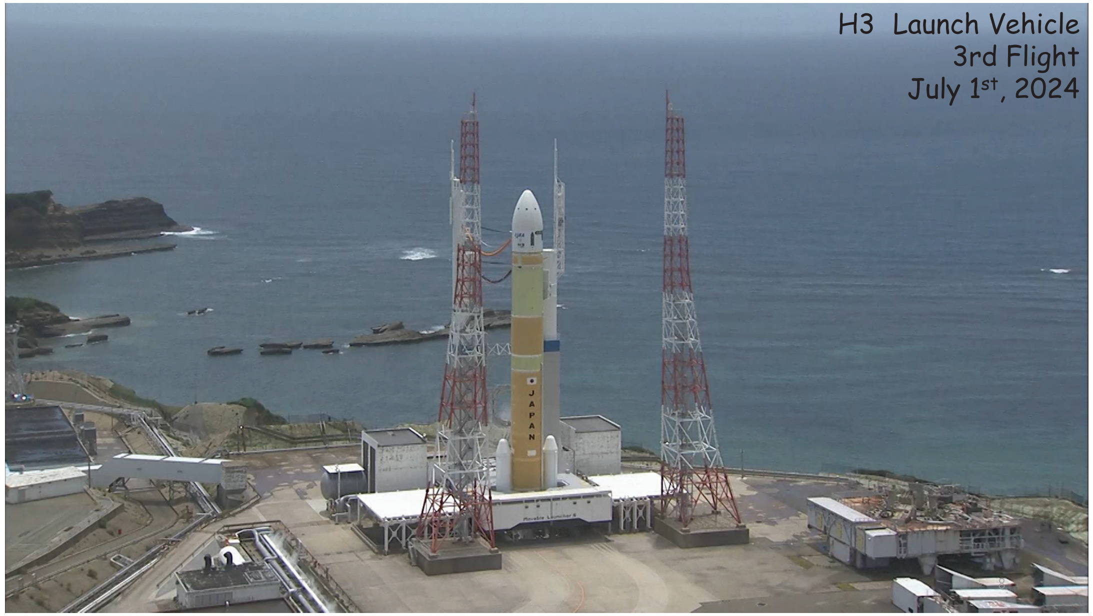

Applications of SLAU type schemes in JAXA's research projects

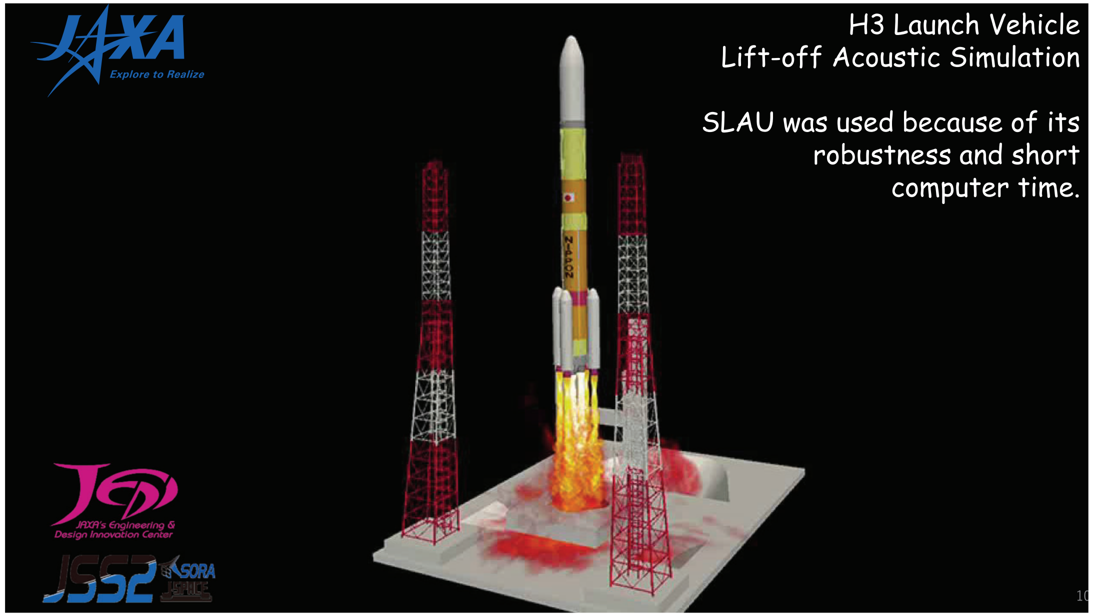

Application of mSLAU for Rotorcrafts(1)

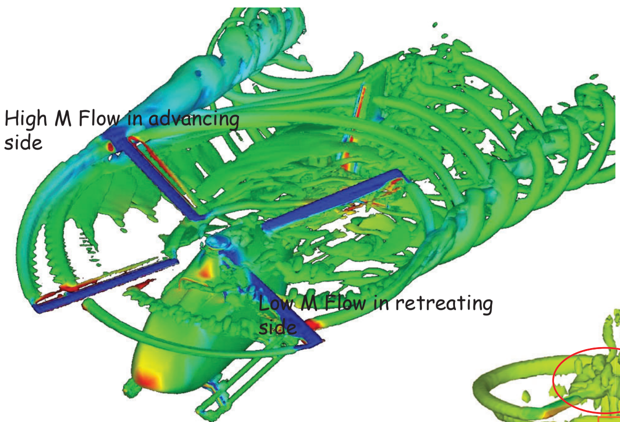

SLAU type schemes are appropriate for rotorcrafts because blades in advancing flight are exposed in high Ma flow at the advancing side and Low Ma flow in the retreating side.

The resolution of the flow field around propellers at low M is improved by mSLAU(modified SLAU)(Tanabe,Y. & Saito,S.,2009)

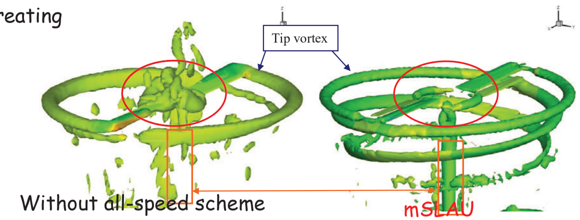

Application of mSLAU for Rotorcrafts(2)

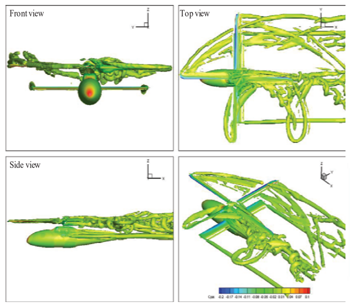

Compound helicopter

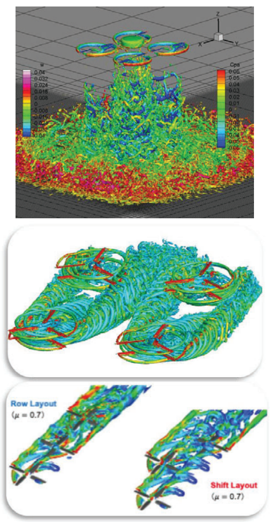

Multirotor EVTOL

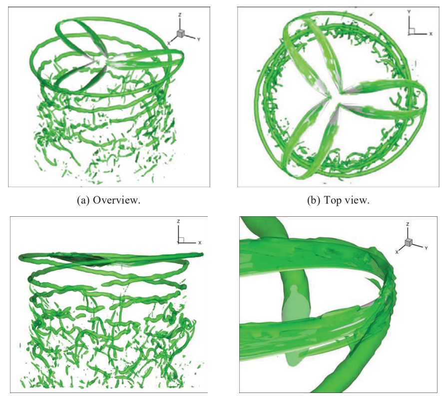

(a) Overview. (b) Top view. (c) Side view. (d) Enlarged view near blade tip.

Low Noise Loop-type Propeller

Numerical Study on Aerodynamic Characteristics of Loop Propeller toward Quiet eVTOL
Yoshiki Nakaniida, Makoto Sato and Eiji Shima

Application of SLAU2 for the combustion

"HINOCA is a CFD solver for detailed simulation of internal combustion engines. The core program is primarily developed in AICE(The Research association of Automotive Internal Combustion Engines), JARI(Japan Automobile Research Institute), JAXA, with sub-models being developed by universities and research institutes in Japan."

Points of HINOCA,

- Density-based compressible flow analysis
  - ✓ The standard for automotive engine simulation is pressure-based flow analysis.
  - ✓ Although most of the flow is at low Ma, it is important to accurately resolve the pressure waves.
  - ✓ SLAU2 is effective for analysis over a wide range of Ma.
- Minimize cost of mesh generation for complex and moving geometry
  - ✓ Cartesian grid
  - ✓ Immersed boundary (IB) method

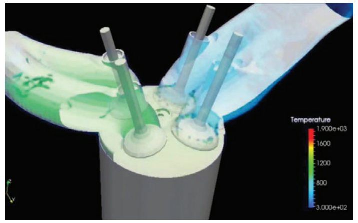

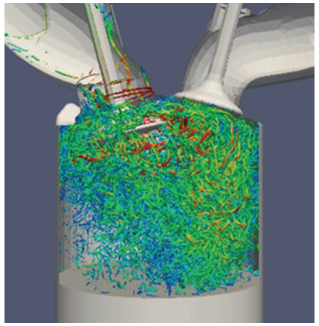

Validations of HINOCA

The variation in cylinder pressure with crank angle change is compared with the results obtained from the one-dimensional analysis software GT-Power, which was tuned to match experimental data.

Motoring analysis of Automotive engine

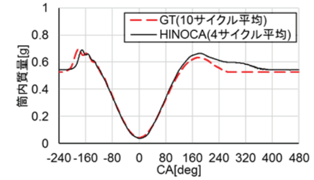

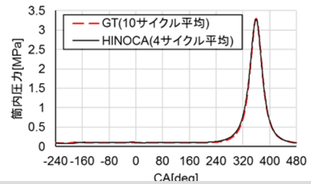

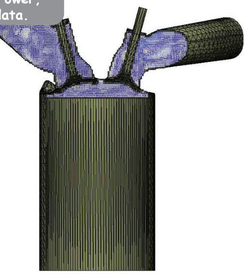

Combustion analysis of JAXA's aircraft engine by HINOCA-AE (Aircraft Engine

Outline of the analysis target

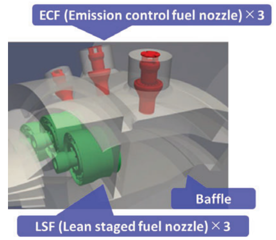

Temperature distributions on the center plain

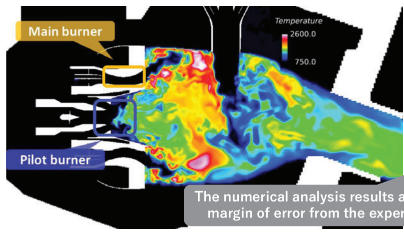

Temperature distributions at the combustor exit

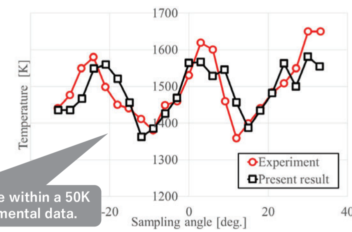

The numerical analysis results are within a 50K margin of error from the experimental data.

Applications of SLAU type schemes(1)

Hypersonic Reentry

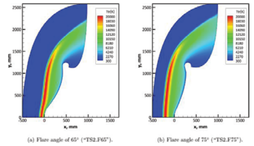

Reentry of Aeroshell
Aerodynamic heating of inflatable aeroshell in orbital reentry
Yusuke Takahashia, Kazuhiko Yamadab(2018)

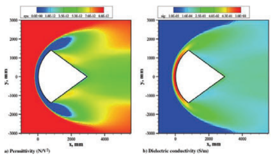

Blackout and Plasma Attenuation
Prediction Performance of Blackout and Plasma Attenuation in Atmospheric Reentry Demonstrator Mission
Yusuke Takahashi, Kazuhiko Yamada and Takashi Abe(2014)

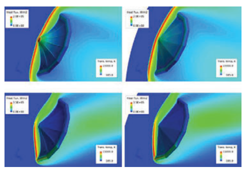

Reentry of Aeroshell
Aerothermodynamic analysis for deformed membrane of inflatable aeroshell in orbital reentry mission
YusukeTakahashia, Taiki Koikea, Nobuyuk iOshimaa, KazuhikoYamadab(2019)

Launch Vehicles aerodynamics

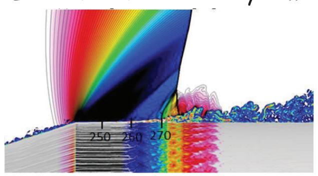

Transonic turbulent flow on Nose Cone
Hybrid LES/RANS Simulations of Transonic Flowfield around a Rocket Fairing
Seiji Tsutsumi, Ryoji Takaki, Yoshiki Takama, Kentaro Imagawa, Kazuyuki Nakakita and Hiroyuki Kato(2012)

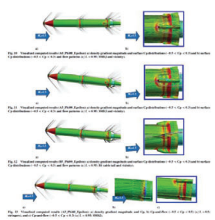

Epsilon Launch Vehicle
Numerical and Experimental Investigations of Epsilon Launch Vehicle Aerodynamics at Mach 1.5
Keiichi Kitamura, Satoshi Nonaka, and Kazuto Kuzuu
Junya Aono, Keiichiro Fujimoto and Eiji Shima(2013)

Applications of SLAU type schemes(2)

LES of Low Ma Flows

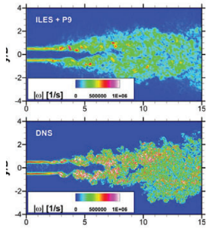

Plane Jet
Implicit large-eddy simulation of turbulent plane jet at Re = 10^4
Shingo Matsuyama(2023)

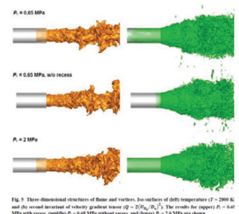

LES of Injector
Validation of LES for High-Pressure Gaseous H2-O2 Coaxial Jet Flame: Comparison with OH-PLIF Measurements
Shingo Matsuyama(2019)

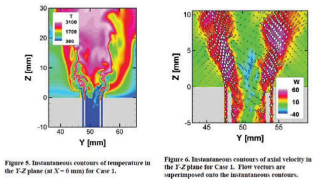

Figure 5. Instantaneous contours of temperature in the Y-Z plane (at X = 0 mm) for Case 1.

Figure 6. Instantaneous contours of axial velocity in the Y-Z plane for Case 1. Flow vectors are superimposed onto the instantaneous contours.

LES of Combustion
Large Eddy Simulation of CH4/O2 Combustion of a Swirl-Coaxial Injector
Shingo Matsuyama(2014)

Hybrid Rocket

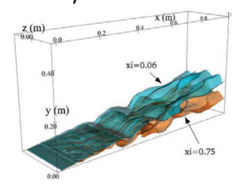

Combustion in hybrid rocket
Polymer Combustion as a Basis for Hybrid Propulsion: A Comprehensive Review and New Numerical Approaches
Vasily Novozhilov, Paul Joseph, Keiichi Ishiko, Toru Shimada, Hui Wang and Jun Liu(2011)

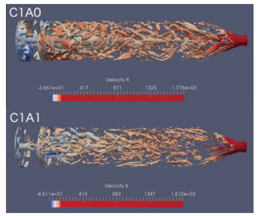

Hybrid Rocket
Numerical Analysis of Combustion Field in Hybrid Rocket Motor with Swirling and Axial Oxidizer Injection
Mikiro Motoe, Tomoki Matsuno and Toru Shimada (2017)

Applications of SLAU type schemes(3)

Hypersonic Intake

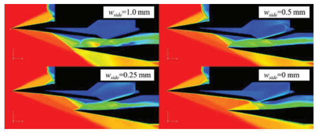

Scram Jet Engine
Numerical Simulation of the Side-Clearance Effect on the Supersonic Air-Inlet Performance for High Mach Integrated Control Experiment "HIMICO"
Masakazu Sano, Hidekazu Yoshida, Sho Wakabayashi, Takahiro Chiga, Tetsuya Sato
Atsushi Hashimoto, and Takayuki Kojima(2018)

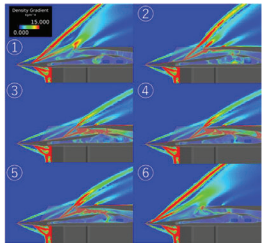

Pre-Cooled Turbo Jet Engine
3-Dimensional Numerical Simulation of Hypersonic Intake for Pre-Cooled Turbo Jet Engine
By Masakazu SANO, Toshiya YOKOI, Hidekazu YOSHIDA, Tetsuya SATO, and Hideyuki TAGUCHI(2019)

Next Generation SST

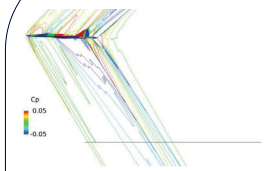

Sonic Boom Wave form
Numerical Simulation of Diffracted U-Shaped Sonic Boom Waveform
Masashi Kanamori, Hiroaki Ishikawa, Yusuke Naka, and Yoshikazu Makino(2022)

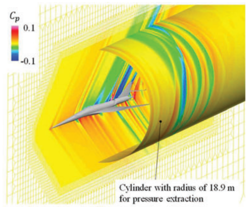

Low Boom Design
Robust Low-Boom Design in Primary Boom Carpet
Atsushi Ueno and Yoshikazu Makino

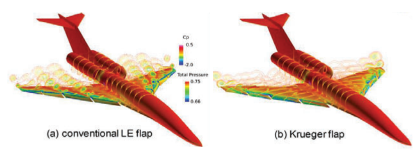

High Lift Devices
PRELIMINARY STUDY OF THE AERODYNAMIC CHARACTERISTICS OF KRUEGER FLAP ON THE SST CONFIGURATION
Dongyoun Kwak*, Keisuke Ohira(2018)

Applications of SLAU type schemes(4)

Electric/Hybrid Aircraft

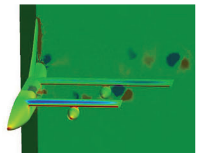

UAV eVTOL
Forward Wing Tip Design for Induced Drag Reduction of Quad Tilt Wing VTOL Un-Manned Plane in Cruise
Yoshihisa Aoki and Koji Muraoka(2019)

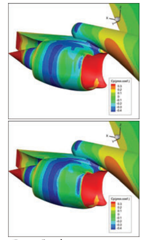

Optimization of Electric Fan Caul of Hybrid Aircraft
Aerodynamic Shape Optimization of Wake Adaptive Thruster on Hybrid-electrified Aircraft with Surrogate Model and Dimension Reduction
Masaya Funada, Keisuke Sugaya, Yuzuru Yokokawa and Hiroshi Kobayashi

Transonic Transport Aircraft

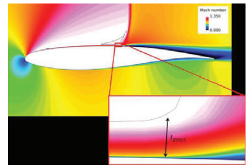

Transonic Buffet
Transonic Buffet Simulation over Supercritical Airfoil by Unsteady FaSTAR Code
Takashi Ishida1, Keiichi Ishiko, Atsushi Hashimoto, Takashi Aoyama(2016)

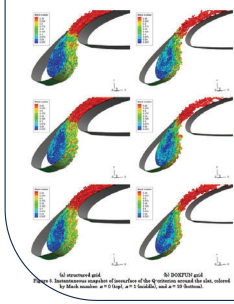

Aeroacoustics of low Ma flow
Slat Noise Simulation on Unstructured Grid with Reduced Dissipation Approach
Ryotaro Sakai, Takashi Ishida, Mitsuhiro Murayama, Yasushi Ito, and Kazuomi Yamamoto(2019)

History and theories

1. What is the Riemann flux function?

FVM(Finite Volume Method) for Navier-Stokes Equation

NS Equation with the Source term in the Static Flame

$$\iiint_\Omega \boldsymbol{Q}_t dV + \iint_{\partial\Omega} \boldsymbol{E} ds - \iint_{\partial\Omega} \boldsymbol{D} ds - \iiint_\Omega \boldsymbol{S}_t dV \boldsymbol{F}_y = 0$$

Conservative Variable | advection | Diffusion | Source

Euler Equation

$$\iiint_\Omega \boldsymbol{Q}_t dV + \iint_{\partial\Omega} \boldsymbol{E} ds = 0$$

FVM Notation

$$\frac{1}{\Delta t}\Delta \bar{\boldsymbol{Q}}_i + \frac{1}{Vi}\sum\left(\bar{\boldsymbol{E}}_{i,j}\Delta s\right) = 0$$

$$\Delta \boldsymbol{Q} \equiv \iiint_\Omega \left(\boldsymbol{Q}^{n+1} - \boldsymbol{Q}^n\right) dV$$

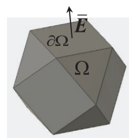

FVM is exact if the face average is exact.

$$\bar{\boldsymbol{E}}_{i,j} = \frac{1}{\Delta t \Delta s_{i,j}} \int_{n\Delta t}^{(n+1)\Delta t} \left(\iint_{\partial\Omega_{i,j}} \boldsymbol{E} ds \right) dt$$

However, obtaining the exact average flux is as difficult as solving Euler equation exactly.
So, we need approximations.

What is the Riemann Flux Function?

- Godunov Scheme (Godunov,S.,1959)
  - Assuming the constant distribution in the cell (control volume), flux can be computed as the solution to the Riemann Initial Value problems.

- The Riemann Flux Function
  - The detail of the solution will be lost, only the influence of the flux at the interface will remain. The flux is called the Riemann flux.
  - I will call the functions that give "appropriate" flux from two independent physical states "The Riemann Flux Function" or "The Riemann Flux".

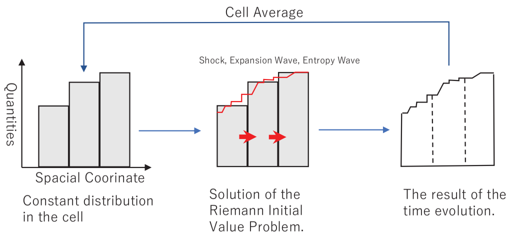

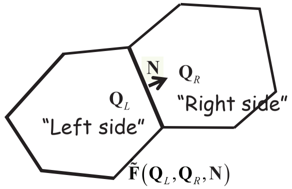

Higher Order Godunov-type Method

- O(Δx) discontinuity at the interface produce the 1st order error.

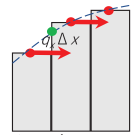

- Higher order accuracy by the reconstruction in the cell can achieved.
  - The distribution of the physical value is reconstructed by some method before the Riemann flux computation. The error at the interface will be reduced.
    →MUSCL (Monotonic Upstream-centered Scheme for Conservation Laws)(van Leer, B.,1979)

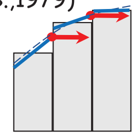

  - Many methods have been developed and studied, and some techniques have become standard, such as MUSCL, TVD, ENO, WENO, etc.
    The details are omitted in this talk.

Higher Efficiency is Achieved by the Implicit Algorism

The Procedure of the Implicit CFD Method for the Compressible Navier-Stokes Equations

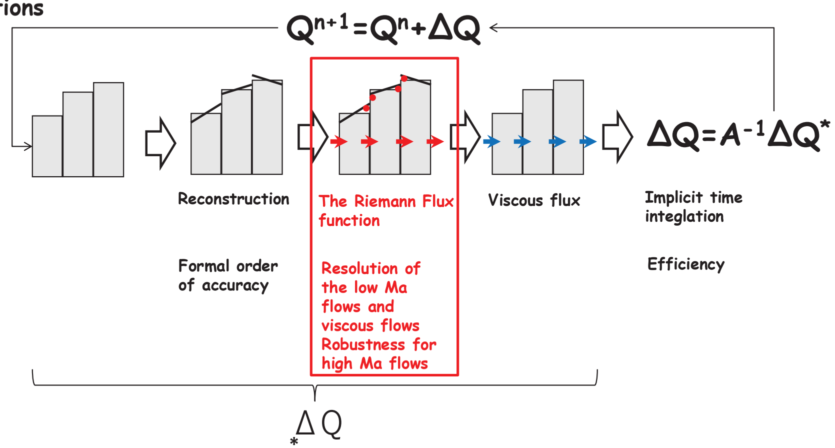

Remarks on the Riemann Fluxes

- The exact solution has little benefit.
  - Although the exact solution can be computed, it is merely an approximation in multidimensional flows or higher-order schemes.
  - The theory is simple, however, the computation is time consuming.
  - The numerical dissipation is too big for low Ma flows.
  - This tend to create anomalies at the shock wave known as the carbuncle phenomena.

- Therefore approximate Riemann fluxes are more attractive.

History and Theories

2. Toward the AUSM type Schemes

Common Form of AUSM type schemes

Flux of the Euler equation in 3-D FVM form can be written as;

$$\hat{\mathbf{E}} = \dot{m}\boldsymbol{\Phi} + p\mathbf{N} \qquad \boldsymbol{\Phi} = \begin{pmatrix} 1 \\ u \\ v \\ w \\ h \end{pmatrix} \qquad \mathbf{N} = \begin{pmatrix} 0 \\ x_n \\ y_n \\ z_n \\ 0 \end{pmatrix} \qquad \dot{m} = \rho V_n \qquad h = \frac{e+p}{\rho}$$

Concentration — Face normal — Mass flux — Total Enthalpy

The flux of AUSM(Liou,M.-S., Steffen Jr.,C.J., 1993) type schemes is close to the definition of the Euler flux.

$$\tilde{\mathbf{E}} = \frac{\dot{m}+|\dot{m}|}{2}\boldsymbol{\Phi}_L + \frac{\dot{m}-|\dot{m}|}{2}\boldsymbol{\Phi}_R + \tilde{p}\mathbf{N}$$

The mass Flux $\dot{m}$ and the interface pressure $\tilde{p}$ are everything for the AUSM type scheme.

I will show how these schemes were made.

CIR(Courant,R., Isaacson,E. & Rees,M. 1952) scheme

The Godunov scheme is the 1st order upwind difference for the Euler Equation.

Here we think about the spatially one-dimensional linear hyperbolic system.

$$\mathbf{Q}_t + \mathbf{A}\mathbf{Q}_x = 0$$

CIR scheme which is 1st order upwind scheme can be written in the FVM form.

$$\mathbf{Q}^{n+1} = \mathbf{Q}^n - \frac{\Delta t}{\Delta x}\left(\tilde{\mathbf{E}}_{i+1/2} - \tilde{\mathbf{E}}_{i-1/2}\right)$$

$$\tilde{\mathbf{E}}_{i+1/2} = \frac{1}{2}\left\{(\mathbf{AQ})_i + (\mathbf{AQ})_{i+1} - |\mathbf{A}|(\mathbf{Q}_{i+1} - \mathbf{Q}_i)\right\}$$

Here we use the following orthogonal transformation.

$$\mathbf{A} = \mathbf{T}\,\mathbf{diag}(\lambda_k)\mathbf{T}^{-1}$$
$$|\mathbf{A}| = \mathbf{T}\,\mathbf{diag}(|\lambda_k|)\mathbf{T}^{-1}$$

Two origins of the approximate Riemann Fluxes: FDS and FVS

CIR

$$\tilde{\mathbf{E}} = \frac{1}{2}\left\{(\mathbf{AQ})_L + (\mathbf{AQ})_R - |\mathbf{A}|(\mathbf{Q}_R - \mathbf{Q}_L)\right\}$$

$\mathbf{E} = \mathbf{AQ}$ — Equivalent in linear case — $\mathbf{A}^{\pm} = \dfrac{\mathbf{A} \pm |\mathbf{A}|}{2}$

$$\tilde{\mathbf{E}} = \frac{1}{2}\left\{\mathbf{E}_L + \mathbf{E}_R - |\mathbf{A}|(\mathbf{Q}_R - \mathbf{Q}_L)\right\} \qquad \tilde{\mathbf{E}} = \mathbf{A}^{+}\mathbf{Q}_L + \mathbf{A}^{-}\mathbf{Q}_R$$

Extension for non-linear equation

$$\tilde{\mathbf{E}} = \frac{1}{2}\left\{\mathbf{E}_L + \mathbf{E}_R - |\tilde{\mathbf{A}}|(\mathbf{Q}_R - \mathbf{Q}_L)\right\} \qquad \tilde{\mathbf{E}} = \mathbf{A}_L^{+}\mathbf{Q}_L + \mathbf{A}_R^{-}\mathbf{Q}_R$$

$\tilde{\mathbf{A}}$: from Roe Averaged Value

FVS(Flux Difference Splitting) (Roe,P.L. 1981)
Drawbacks: Strong shock and expansion

FVS(Flux Vector Splitting)
(Steger,J.L.&Warming,R.F, 1979)
Drawbacks: Large error at contact surface

Improvement of FVS(van Leer,B.,1982)

Challenge: Avoiding glitches in SW-FVS

- Smooth transition at switching using polynomials is introduced.
- Simpler form than SW-FVS was achieved.

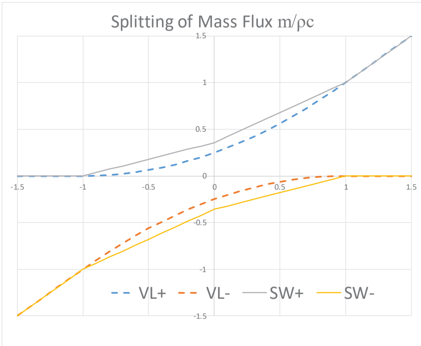

Improvement of FVS (Hänel & Schwane,1989)

Challenge： Preservation of total enthalpy which is crucial in high Ma flows

The vL-FVS can be rewritten to separate contributions of advection and pressure.

$$_{vL}\widetilde{\mathbf{E}} = {}_{vL}\widetilde{\mathbf{E}}_L^+ + {}_{vL}\widetilde{\mathbf{E}}_R^- \qquad {}_{vL}\widetilde{\mathbf{E}}^\pm = \dot{m}^\pm \mathbf{\Phi}' + p^\pm \mathbf{N}$$

$$\mathbf{\Phi}'_L = \mathbf{\Phi}_L + \left(0,0,0,0,-\frac{(V_{nL}-c_L)^2}{\gamma+1}\right)^T \qquad \mathbf{\Phi}'_R = \mathbf{\Phi}_R + \left(0,0,0,0,-\frac{(V_{nR}+c_R)^2}{\gamma+1}\right)^T$$

Preservation of total enthalpy is improved by small change in the energy term.
→Hänel's FVS

$$_{Hanel}\widetilde{\mathbf{E}} = \widetilde{\mathbf{E}}_L^+ + \widetilde{\mathbf{E}}_R^- \qquad \widetilde{\mathbf{E}}^\pm = \dot{m}^\pm \mathbf{\Phi} + p^\pm \mathbf{N}$$

Very close form to the definition of the Euler flux.

Improvement of FVS (cont'd)

By separating the flux to the advection and the pressure term, it was found that interface pressure can be written in the weighted average of the pressure on the left and right.

$$\widetilde{p} = p_L^+ + p_R^- = p_L \beta_L^+(M_L) + p_R \beta_R^-(M_R)$$

Although it became clear by Hänel's modification, it has been included in the van Leer's FVS.
We will keep using this interface pressure in AUSM type schemes.

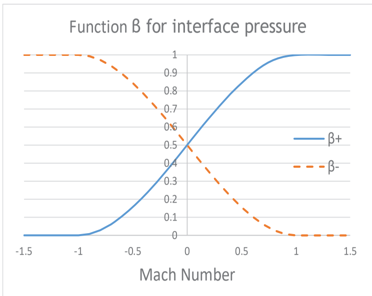

From FVS to AUSM

Challenge: Accuracy for contact surfaces and viscous flows

AUSM is well known, however, here we explain using the concept of SFS(Simplified Flux Vector Splitting).(Jounouchi,T. et al.. 1991)
Hänel's FVS can be written as follows.

$$_{Haenel}\widetilde{\mathbf{E}} = {}_{vL}\dot{m}_L^+ \mathbf{\Phi}_L + {}_{vL}\dot{m}_R^- \mathbf{\Phi}_R + \widetilde{p}\mathbf{N}$$

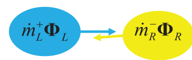

In this form, particles from each side transport the concentration of each side independently.
This works as numerical molecular diffusion and is not the correct behavior of the Euler flux.
If the fluid as a particle transports the concentration, one particle on the upwind side should do.

$$_{SFS}\dot{m} = \dot{m}_L^+ + \dot{m}_L^-$$

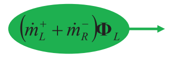

$$_{AUSM-F}\widetilde{\mathbf{E}} = \frac{\dot{m}+|\dot{m}|}{2}\mathbf{\Phi}_L + \frac{\dot{m}-|\dot{m}|}{2}\mathbf{\Phi}_R + \widetilde{p}\mathbf{N}$$

The common form of the AUSM type schemes is obtained.

Common Form of AUSM type schemes

$$\tilde{\mathbf{E}} = \frac{\dot{m}+|\dot{m}|}{2}\mathbf{\Phi}_L + \frac{\dot{m}-|\dot{m}|}{2}\mathbf{\Phi}_R + \tilde{p}\mathbf{N}$$

The mass flux and the interface pressure are everything for the AUSM type scheme.

33

History and Theories

3. Toward the All-Speed Schemes (1)Interface Pressure

The interface pressure also works as the numerical dissipation and needs to be adjusted for low M flows.

34

Numerical Dissipation in the Interface Pressure

AUSM type schemes inherit the interface pressure from van Leer 's FVS

$$\tilde{p} = \beta^+ p_L + \beta^- p_R$$

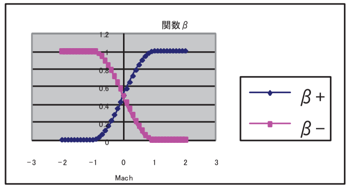

Exactly rewritten as;

$$\tilde{p} = \frac{p_L+p_R}{2} + \frac{\beta^+-\beta^-}{2}(p_L-p_R) + \left(\beta^+ + \beta^- - 1\right)\frac{p_L+p_R}{2}$$

M<<1 →

$$\frac{3}{4\gamma}\frac{\rho_L+\rho_R}{2}\bar{c}(V_{nL}-V_{nR})$$

This term works as numerical bulk viscosity with the scale of the sound speed. The scale is good only for the flow at near-sound speed.

35

Controlling the Numerical Dissipation

Control the scale of dissipation by smooth function of Ma.

$$\tilde{p} = \frac{p_L+p_R}{2} + \frac{\beta^+-\beta^-}{2}(p_L-p_R) + \left(\beta^+ + \beta^- - 1\right)\frac{p_L+p_R}{2}$$

(Shima,E.,2006)

$$\tilde{p} = \frac{p_L+p_R}{2} + \frac{\beta^+-\beta^-}{2}(p_L-p_R) + \kappa\left(\beta^+ + \beta^- - 1\right)\frac{p_L+p_R}{2}$$

(Ma)x(Sound Speed) = Advective Speed

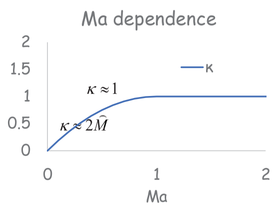

$$\kappa = 1-(1-\hat{M})^2 = 2\hat{M} - \hat{M}^2$$

$$\hat{M} = \min\left(1.0, \frac{1}{\bar{c}}\sqrt{\frac{u^{+2}+v^{+2}+u^{-2}+v^{-2}}{2}}\right)$$

36

Choice of the interface Ma

The use of the multidimensional Mach number gives good solution.

Pressure Distribution NACA0012 M_∞=0.6 α=5° Inviscid

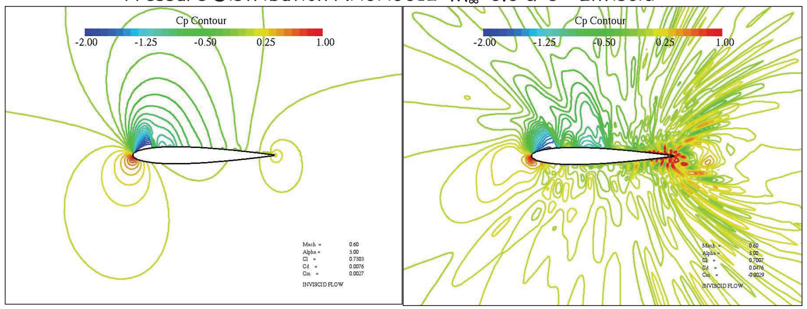

Multidimensional Mach Number	One Dimensional Mach Number
$\hat{M} = \min\left(1.0, \frac{1}{\bar{c}}\sqrt{\frac{u^{+2}+v^{+2}+u^{-2}+v^{-2}}{2}}\right)$	$\hat{M} = \min\left(1.0, \frac{1}{\bar{c}}\sqrt{\frac{V_n^{+2}+V_n^{-2}}{2}}\right)$

Non-physical drag divergence at low Ma was corrected by SLAU.

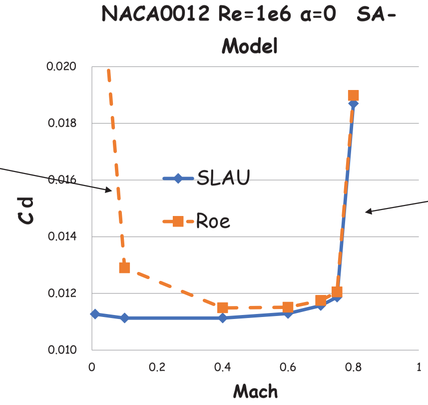

Non-physical drag divergence at low Ma

Physical drag divergence at transonic speed

Improved Resolution for Viscous Flows M_∞=0.01 Re=10^6

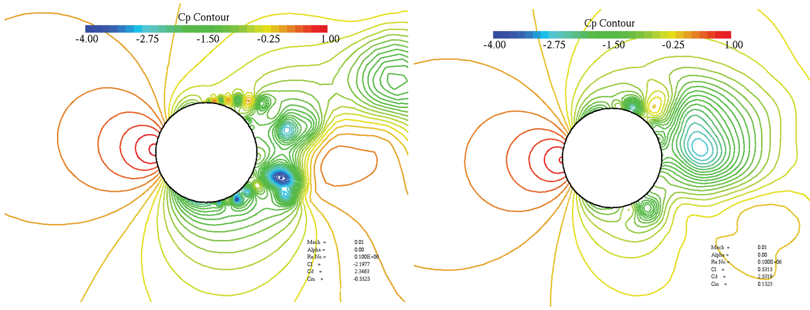

SLAU 3rd order without limiter MFGS implicit scheme

Roe scheme 3rd order without limiter MFGS implicit scheme

SLAU2 for hypersonic and general EOS

AUSM

$$\tilde{p} = \beta^+ p_L + \beta^- p_R = \frac{p_L + p_R}{2} + \frac{\beta^+ - \beta^-}{2}(p_L - p_R) + (\beta^+ + \beta^- - 1)\frac{p_L + p_R}{2}$$

Change the scale of the dissipation at Low Ma.

SLAU (Shima,E.,2008)

$$\tilde{p} = \frac{p_L + p_R}{2} + \frac{\beta^+ - \beta^-}{2}(p_L - p_R) + \kappa(\beta^+ + \beta^- - 1)\frac{p_L + p_R}{2}$$

Too small for the hypersonic speed

It only work as proper dissipation when p≈ρc²

SLAU2 (Kitamura.K. & Shima.e.,2011)

$$\tilde{p} = \frac{p_L + p_R}{2} + \frac{\beta^+ - \beta^-}{2}(p_L - p_R) + \hat{M}(\beta^+ + \beta^- - 1)\overline{\rho c}^2$$

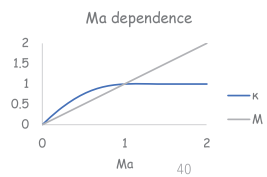

History and Theories

3. Toward the All-Speed Schemes (2)Mass Flux

The pressure difference term in the mass flux works as the dissipation for the acoustic wave.
But it also causes the carbuncle phenomena.

Early AUSM type schemes inherit the mass flux of FVS.

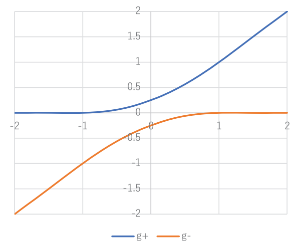

FVS $\quad {}_{FVS}\dot{m} = g^{+}(M_L)\rho_L c_L + g^{-}(M_R)\rho_R c_R$

SFS $\quad {}_{SFS}\dot{m} = g^{+}(M_L)\rho_L \bar{c} + g^{-}(M_R)\rho_R \bar{c}$

AUSM

$$\bar{M} = g^{+}(M_L) + g^{-}(M_R)$$

$${}_{AUSM}\dot{m} = \frac{\bar{M}+|\bar{M}|}{2}\rho_L \bar{c} + \frac{\bar{M}-|\bar{M}|}{2}\rho_R \bar{c}$$

$$g^{\pm}(M) = \begin{cases} \pm\frac{1}{4}(M\pm 1)^2 & if\ |M|<1, \\ \frac{1}{2}(M \pm |M|) & otherwise \end{cases}$$

AUSM-DV
(Wada,Y.,1997)

$${}_{AUSM-DV}\dot{m} = \rho_L\left\{\alpha_L \frac{V_{nL}+|V_{nL}|}{2} + (1-\alpha_L)g^{+}(M_L)c_L\right\} + \rho_R\left\{\alpha_R \frac{V_{nR}-|V_{nR}|}{2} + (1-\alpha_R)g^{-}(M_R)c_R\right\}$$

Utilize the Mass Flux of FDS

They were natural choices. However, the mass flux of FDS is better to control term by term.

SHUS(Simple High-resolution Upwind Scheme) (Shima,E. et al., 1994)

$$\dot{m} = \frac{1}{2}\left\{(\rho V_n)_L + (\rho V_n)_L - |\bar{V}_n|\Delta\rho - \frac{|\bar{M}+1|-|\bar{M}-1|}{2}\bar{\rho}\Delta V_n - \frac{|\bar{M}+1|+|\bar{M}-1|-2|\bar{M}|}{2\bar{c}}\Delta p\right\}$$

The mass flux of FDS

$$\Delta q \equiv q_R - q_L$$

For very low M, the mass flux approaches to;

$$\bar{M} \to 0$$

$$\dot{m} = \frac{1}{2}\left\{(\rho V_n)_L + (\rho V_n)_L - |\bar{V}_n|\Delta\rho - \frac{1}{\bar{c}}\Delta p\right\}$$

For acoustic wave, the last term works as dissipation.

$$\Delta p = \bar{c}^2\Delta\rho$$

$$\dot{m} = \frac{1}{2}\left\{(\rho V_n)_L + (\rho V_n)_L - \left(\bar{c} + |\bar{V}_n|\right)\Delta\rho\right\}$$

Effect of the Pressure Difference Term

Here we will see the effect of the pressure difference term.

SHUS

$$\dot{m} = \frac{1}{2}\left\{(\rho V_n)_L + (\rho V_n)_L - |\bar{V}_n|\Delta\rho - \frac{|\bar{M}+1|-|\bar{M}-1|}{2}\bar{\rho}\Delta V_n - \boxed{\frac{|\bar{M}+1|+|\bar{M}-1|-2|\bar{M}|}{2\bar{c}}\Delta p}\right\}$$

The Δp term in the mass flux will cause the carbuncle at shockwave.
(Liou,M.-S.,2000)

ST(Simplest)-AUSM(Shima,E.,2000)

$$\dot{m} = \frac{1}{2}\left\{(\rho V_n)_L + (\rho V_n)_L - |\bar{V}_n|\Delta\rho\right\}$$

No Pressure Difference Term

Both schemes work well in general. The Δp term can eliminate noise in low Ma but cause the carbuncle in supersonic.

	Δp	M>1	M<<1
SHUS	ON	NG Carbuncle 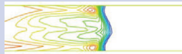	Good 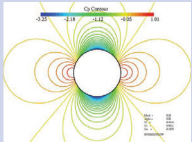
ST-AUSM	OFF	Good No carbuncle	NG 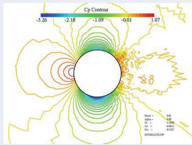

Review of Mass Flux of SHUS at the Shock Wave

Review of the Δp term of SHUS at the shock wave.

$$\dot m = \frac{1}{2}\left\{(\rho V_n)_L + (\rho V_n)_L - |\bar V_n|\Delta\rho - \frac{|\bar M+1| - |\bar M-1|}{2}\bar\rho\Delta V_n - \frac{|\bar M+1| + |\bar M-1| - 2|\bar M|}{2\bar c}\Delta p\right\}$$

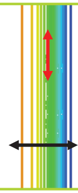

Along the shockwave, only Δp remains.

$\bar M \approx 0 \quad \dot m \approx -\frac{1}{2c}\Delta p$

Across the shockwave, no Δp.

$\bar M \approx 1 \quad \dot m = \frac{1}{2}\{(\rho V_n)_L + (\rho V_n)_L - |\bar V_n|\Delta\rho\}$

The Δp term along the shockwave causes the carbuncle phenomena.

Mass Flux for SLAU

We will see the effect of the pressure difference term.

SHUS

$$\dot m = \frac{1}{2}\left\{(\rho V_n)_L + (\rho V_n)_L - |\bar V_n|\Delta\rho - \frac{|\bar M+1| - |\bar M-1|}{2}\bar\rho\Delta V_n - \boxed{\frac{|\bar M+1| + |\bar M-1| - 2|\bar M|}{2\bar c}\Delta p}\right\}$$

$\Delta q \equiv q_R - q_L$

ST-AUSM

$$\dot m = \frac{1}{2}\{(\rho V_n)_L + (\rho V_n)_L - |\bar V_n|\Delta\rho\}$$

SLAU(Shima,E.,2008)

$$\dot m = \frac{1}{2}\left\{(\rho V_n)_L + (\rho V_n)_L - |\bar V_n|\Delta\rho - \boxed{(1-\kappa)\frac{1}{c}\Delta p}\right\}$$

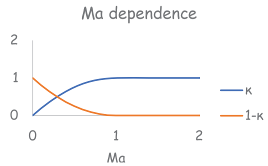

Simply eliminates in whole high Ma region.

$$1-\kappa = (1-\hat M)^2 \quad \hat M = \min\left(1.0, \frac{1}{\bar c}\sqrt{\frac{u^{+2}+v^{+2}+u^{-2}+v^{-2}}{2}}\right)$$

The final mass flux of SLAU includes the term $\dot m = \frac{1}{2}\left[\{(\rho V_n)_L + (\rho V_n)_L\}(1-g) - |\bar V_n|\Delta\rho - (1-\kappa)\frac{1}{c}\Delta p\right]$ for strong expansion, but I omit it now. $g = -\max(-1, \min(M_L, 0))\min(1, \max(M_R, 0))$

SLAU is good in both low and high Ma.

	Δp		M>1	M<<1
	High M	Low M		
SHUS	ON	ON	NG Carbuncle 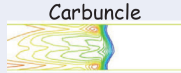	Good 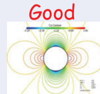
ST-AUSM	OFF	OFF	Good No carbuncle	NG 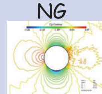
SLAU	OFF	ON	Good No carbuncle	Good 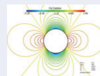

The carbuncle phenomena are more harmful in complex flow fields.

Double Mach Reflection

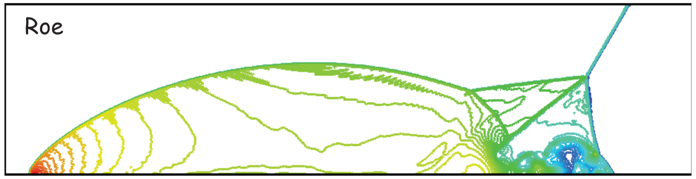

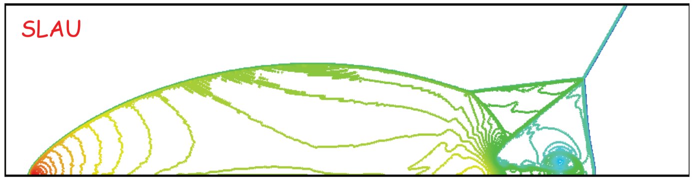

The Shock Layer is a Fictitious Space

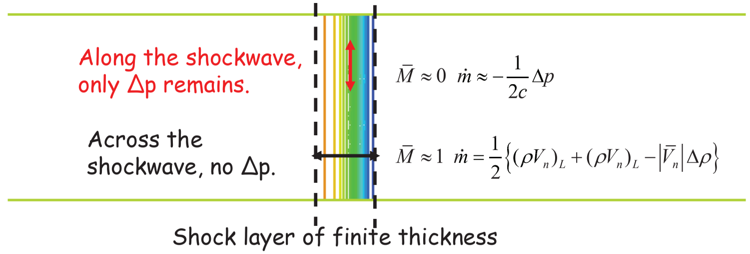

As the behavior of these pressure differences are those of the Euler equation, they must be physically correct.

However, the shock layer of finite thickness is not a physical space. Computing correctly in the fictitious space seems to cause problem.

Therefore better scheme will be achieved, if the pressure difference is eliminated only in the shock layer.

Improved mass flux of SD-SLAU(Shima,E. et al., 2010)

The mass flux of SD(Shock Detecting)-SLAU is defined as;

$$\dot{m} = \frac{1}{2}\left\{\rho^+ V_n^+ + \rho^- V_n^- - |\bar{V}_n|\Delta\rho - \theta(\Delta p/p)\frac{|M+1|+|M-1|-2|M|}{2\bar{c}}\Delta p\right\}$$

Switching function θ is designed to be;

$$\theta\left(\frac{\Delta p}{p}\right)\begin{cases}\approx 0 & \text{in parallel direction to the shock}\\ \approx 1 & \text{otherwise}\end{cases}$$

Basic mass flux 2 : SLAU

$$\dot{m} = \frac{1}{2}\left\{\rho^+ V_n^+ + \rho^- V_n^- - |\bar{V}_n|\Delta\rho - \frac{\chi}{\bar{c}}\Delta p\right\}$$

Basic mass flux 1 : SHUS

$$\dot{m} = \frac{1}{2}\left\{\rho^+ V_n^+ + \rho^- V_n^- - |\bar{V}_n|\Delta\rho - \frac{|\bar{M}+1|-|\bar{M}-1|}{2}\bar{\rho}\Delta V_n - \frac{|\bar{M}+1|+|\bar{M}-1|-2|\bar{M}|}{2\bar{c}}\Delta p\right\}$$

Shock Detecting Function

Actual form of fp is;

$$f_p(\Delta p/p) = \min\left(1, \left(\frac{C_{SD2}|\Delta p|/\bar{p} + C_{SD1}}{|\Delta p|_{\max}/\bar{p} + C_{SD1}}\right)^2\right)$$

$C_{SD2} \approx 10$

$C_{SD1} \approx 0.1$

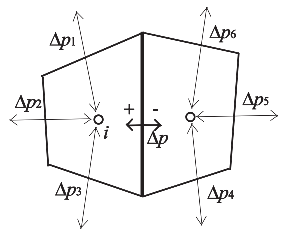

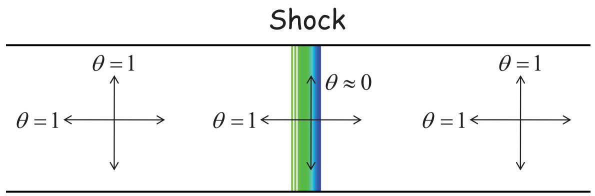

1D shock propagation in distorted 2D channel with distorted mesh

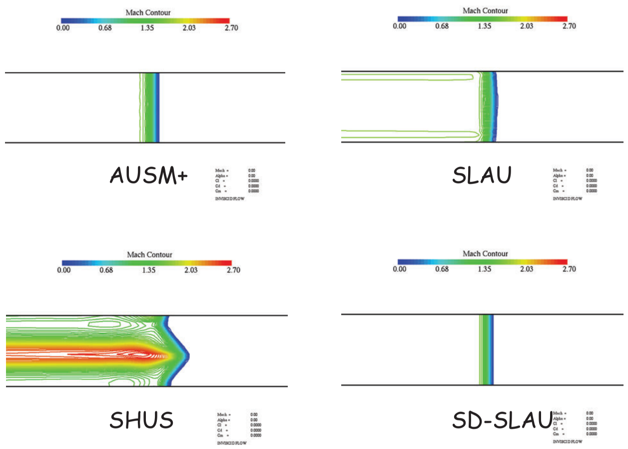

Oblique shock around a thin plate M=6 α=5°

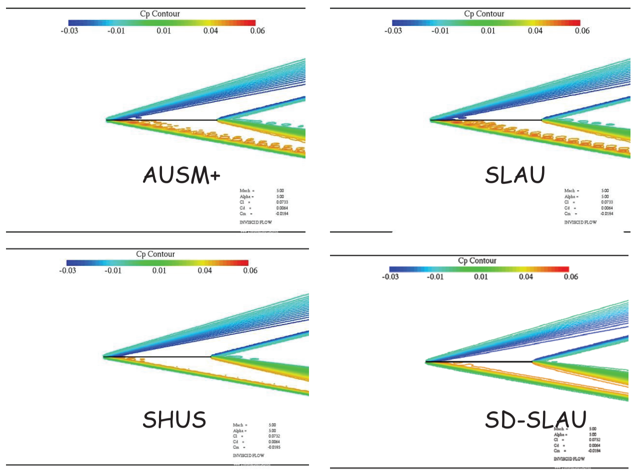

Other Choices for Δp term

The general form of the SLAU type schemes

$$\dot{m} = \frac{1}{2}\left\{(\rho V_n)_L + (\rho V_n)_L - \left|\bar{V}_n\right|\Delta\rho - \boxed{f_p}\frac{1}{c}\Delta p\right\}$$

scheme	f_p	Advantages	Drawback
SLAU	$1-\kappa$		
SD-SLAU	$\min\left(1,\left(\frac{C_{SD2}\lvert\Delta p\rvert/\bar{p}+C_{SD1}}{\lvert\Delta p\rvert_{\max}/\bar{p}+C_{SD1}}\right)^2\right)\max\left(0,1-\lvert\bar{M}\rvert\right)$	Eliminating noise in supersonic flows	More complex
No-name	$\frac{1-\kappa}{\kappa+M_c}$	Monotonic even in low Ma (Ma>Mc)	CFL restriction Cut-off Ma Dissipation of sound
WS(Wiggle Sensing)-SLAU(Shima,E. et al., 2013)	$\left\{1+\min\left(1,C_{ws}\frac{\max\left(\lvert(\bar{\Delta}\bar{\Delta}p)_L\rvert,\lvert(\bar{\Delta}\bar{\Delta}p)_R\rvert\right)}{\max\left(\lvert(\bar{\Delta}p)_L\rvert,\lvert(\bar{\Delta}p)_R\rvert,\varepsilon\right)}\right)\frac{1-\kappa}{\kappa+M_c}\right\}(1-\kappa)$	Eliminating wiggles in very low Ma flows	CFL restriction Cut-off Ma More complex
UD(Uniformly Damping)-SLAU(Shima,E. et al., 2015)	$(1-\kappa)\max\left(1,\frac{\bar{c}T_c}{\Delta x}\right)$	Eliminating unnecessary acoustic wave in low Ma	Needs GC-SMAC

We have better schemes for extreme conditions, however, don't have a simple and universal scheme yet.
SLAU is the simplest and works well in most aerodynamic flows.

Time Integration Method for All Ma

Note on Time Integration Methods

- Time step restriction from CFL condition is severe for low Ma flows due to large ratio of the sound speed to the advection speed.
- The regular implicit time integration methods such as LU-SGS is effective for Ma>0.1. Therefore such schemes are good enough for most aerodynamic flows
- The preconditioning methods as the implicit time integration work well in Ma<0.1 for steady flows.
  However, the choice of cut-off Ma is difficult and they causes storing dissipation on the sound wave propagation.
- *GC*(*Generalized Compressible*)-*SMAC*(Simplified Marker and Cell Method)(Shima,E., etc.,2018), which smoothly approaches to *SMAC* for the incompressible flows in very low Ma, seems promising.

Convert R.H.S. residual to the entropy variable

Use the MUSCL FVM for conservative variables with all speed Riemann flux for R.H.S. evaluation.

$$\overline{\mathbf{Q}}_t + \frac{1}{V_i}\sum_j (\widetilde{\mathbf{E}}_{i,j} - \widetilde{\mathbf{R}}_{i,j}) ds_{i,j} = 0$$

Use the working variables for L.H.S. evaluation for simplicity. Variation of working variables are is obtained by mapping;

$$\delta \mathbf{q}^* \equiv \frac{\partial \mathbf{q}}{\partial \mathbf{Q}}\left[-\delta t \frac{1}{V_i}\sum_j (\tilde{\mathbf{E}}_{i,j} - \tilde{\mathbf{R}}_{i,j}) ds_{i,j} \right]$$

After approximate matrix inversion in working variables, variation of conservative variables is obtained by reverse mapping;

$$\delta \mathbf{Q} \equiv \frac{\partial \mathbf{Q}}{\partial \mathbf{q}} \mathbf{B}^{-1} \delta \mathbf{q}^*$$

Focuses on the evaluation of the inviscid terms, since we treat the viscosity term in regular way,

The Equation become simple in the entropy variables.

Use entropy variables (velocity, pressure, entropy) as working variables. Compressible NS equations using them are written as;

$$\mathbf{u}_t + \mathbf{u}\cdot\nabla\mathbf{u} + \frac{1}{\rho}\nabla p + \mathbf{R}_u = 0$$

$$p_t + \mathbf{u}\cdot\nabla p + \rho c^2 \nabla\cdot\mathbf{u} + R_p = 0$$

$$s_t + \mathbf{u}\cdot\nabla s + R_p = 0$$

Semi-discretize in time to the δ form using the first order implicit method.

$$\delta\mathbf{u} + \delta t\left\{ \mathbf{u}\cdot\nabla\delta\mathbf{u} + \frac{1}{\rho}\nabla\delta p + \frac{\partial \mathbf{R}_u}{\partial \mathbf{u}}\delta\mathbf{u} \right\} = \delta\mathbf{u}^*$$

$$\delta p + \delta t\left\{ \mathbf{u}\cdot\nabla\delta p + \rho c^2 \nabla\cdot\delta\mathbf{u} + \frac{\partial R_p}{\partial p}\delta p \right\} = \delta p^*$$

$$\delta s + \delta t\left\{ \mathbf{u}\cdot\nabla\delta s + \frac{\partial R_s}{\partial s}\delta p \right\} = \delta s^*$$

Operator splitting of least error create SMAC like scheme

L.H.S operator is splitting in the least error manner. The linear equation for the pressure can be solved by similar way as SMAC method for incompressible CFD.

$$\frac{\partial \mathbf{Q}}{\partial \mathbf{q}}\left[\mathbf{I} + \delta t'\,{}_u\mathbf{A}_u\right]\left[\mathbf{I} + \delta t'\left\{{}_u\mathbf{A}_p + {}_p\mathbf{A}_p + {}_p\mathbf{A}_u\right\}\right]\frac{\partial \mathbf{q}}{\partial \mathbf{Q}}\Delta\mathbf{Q} = \mathbf{Q} - \theta_1\mathbf{Q}^n + \theta_2\mathbf{Q}^{n-1} - \delta t'\frac{1}{\Omega_i}\sum_j(\tilde{\mathbf{E}}_{i,j} - \tilde{\mathbf{R}}_{i,j})dS_{i,j}$$

Advection　　Pressure

$$(\theta_1, \theta_2) = \left(\frac{2\theta + 2}{\theta + 2}, \frac{\theta}{\theta + 2} \right)$$

$$\delta t' = \frac{2}{\theta + 2}\delta t$$

$$\theta = \begin{cases} 0 & \text{: First order accuracy} \\ 1 & \text{: Second order accuracy} \end{cases}$$

Appling this operator splitting, the pressure part can be solved by the similar method as SMAC.

Inviscid flow at M = 0.1 around NACA0012
Convergence history of velocity residuals

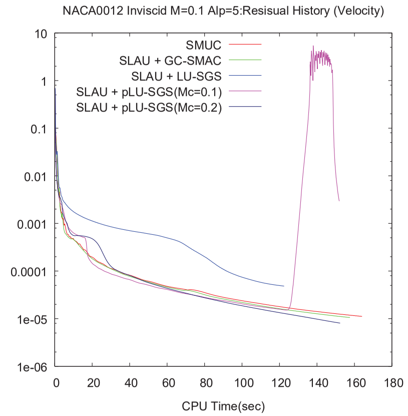

- *SMUC* (UD-SLAU + *GC- SMAC*) is the fastest
- Pre-conditioned LU-SGS(*pLU-SGS*) is also fast, but is sensitive to Mc(Cut-off Mach number).

Inviscid flow at M = 0.01 around NACA0012
Convergence history of velocity residuals

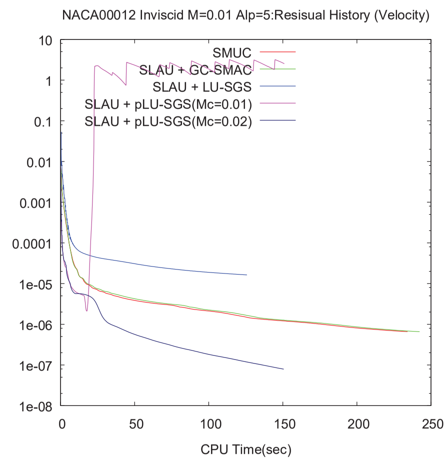

- *pLU-SGS* is the fastest, but is sensitive to Mc.
- *GC-SMAC* is stably fast.

1D Sound Propagation Simulating Sound Emitted From B.L. (CFLmax=10^4)

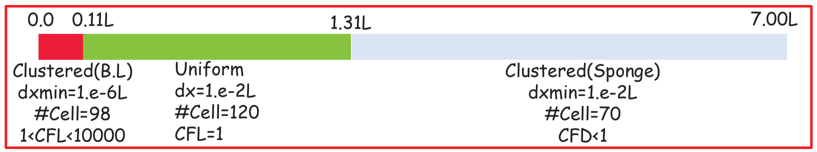

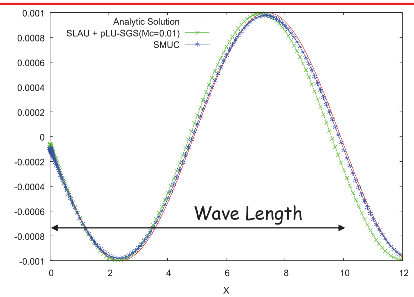

L:Wave Length

Label	-	SLAU+pLU-SGS(Mc=0.01)	-	SMUC
Flux	SLAU	SLAU	SLAU	UD-SLAU
Integration	TVD-RK3	*pLU-SGS*	*GC-SMAC*	*GC-SMAC*
Max. CFL	1	1.00E+04	1.00E+04	1.00E+04
#Newton it.	-	32000	1000	1000
Rel. CPU	9.96	19.26	0.99	1.00

SMUC is 10 times faster than the explicit scheme and 19 times faster than the time derivative pre-conditioned scheme (*pLU-SGS*) with Mc=0.01.
The result of *pLU-SGS* show small deviation even after 32000 Newton iterations.

Future Challenges

- Robustness
  - SLAU works fine with FR for LES alone, however, breakdowns with the combustion. On the other hand, non all-speed SHUS works.
    We don't know why and how to fix.
- Accuracy
  - Utilizing the flexibility of the SLAU type scheme, such as choice of the some averaged values in the scheme or choice of the reconstruction scheme, new features like conservation of the kinetic energy or entropy might be possible.
- Efficiency
  - *GC*(*Generalized Compressible*)-*SMAC* works fine for very low *Ma* without adjustment of the cut-off *Ma* in the trial cases. As the present version is still primitive stage, future researches are expected.

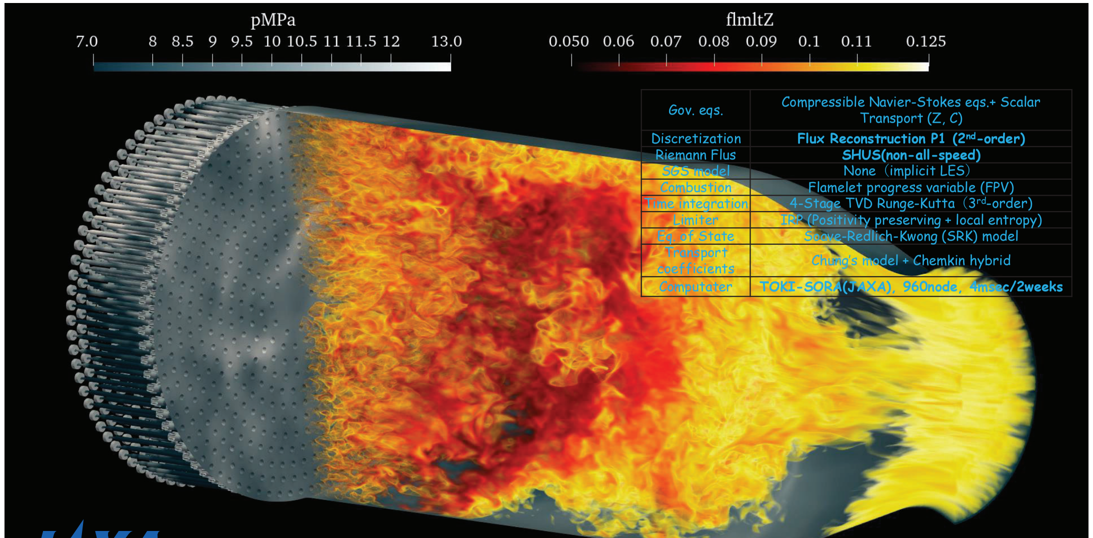

LES of combustion in the full-scale liquid rocket engine
(The Riemann Flux we developed is used, but is not all-speed scheme)

Characteristics of the Riemann Fluxes

	Godunov (Exact Riemann Flux)	Roe (Approximate Riemann Flux)	FVS (Approximate Riemann Flux)	SLAU
Theory	Simple	Simple	Simple	Complex
Cost	NG -Iteration	NG -Orthogonal decomposition	Good	Good
Supersonic(Ma>2)	NG -Carbuncle	NG -Carbuncle -Breakup at strong expansion	Good	Good
Low Ma(<0.1)	NG -Too dissipative	NG -Too dissipative	NG -Too dissipative	Good
Moderate Ma (0.1<Ma<2)	Good	Good	Good	Good
Viscous flow	Good	Good	NG -Too dissipative	Good

Remarks on compressible CFD schemes

•The problem of compressible CFD schemes on computation of low Ma flows have been almost solved.

- •Large numerical dissipation.
  - •Solved by all-speed Riemann fluxes.
- •Strict time step size restriction
  - •In Ma > 0.1, popular and simple implicit time integration schemes, such as LU-SGS, work well.
  - •For lower Ma, the preconditioning methods are effective.
  - •Even in Ma<0.01, efficient methods have been constructed. (such as, *GC-SMAC*, Shima.E.,2015)
- •Roundoff error due to small change.
  - •Can be solved by separating the derivations from the uniform values. In most aerospace applications, the double precision variables are good enough.

Acknowledgments

I am grateful to K. Kitamura for co-authoring several papers on SLAU type scheme.
I would like to thank Dr.Y.Tanabe, Dr.H.Sugawara and Dr.K.Yasue for preparing examples of applications in JAXA.
I would also like to take this opportunity to thank Prof. T.Matsuda, Prof. K.Sawada, Prof. K.Fujii, Prof. T.Jounouchi., Prof.M.-S. Liou, Dr. and Y.,Wada for valuable discussions on the CFD schemes.

Thank you for your attention!